

Supporting Information

New perspective on the laser initiation for metal tetrazine complexes: a theoretical study

Junqing Yang^{a,b,*}, Gu-Dan Zhang^b, Jian-Guo Zhang^{b,*}, Dong Chen^c, Qi Zhang^c

^a School of Mechanical Engineering, Nanjing University of Science and Technology, Nanjing, 210094, China

^b State Key Laboratory of Explosion Science and Technology, Beijing Institute of Technology, Beijing, 100081, China

^c Institute of Chemical Materials, China Academy of Engineering Physics, Mianyang, Sichuan, 621900, China

Table of content:

The mathematical forms for the parameters Sr, D, and t:	S2
Table S1. Excitation descriptors (Sr , D , Sr/D , and t) and the statistical charge transfer data.	S3
Figure S1. UV-vis spectra of NO_3^- (solid line) and non- NO_3^- (dotted line) bounded complexes.	S4
Figure S2. Charge density difference (CDD) plots of complexes 11B-13B and 7B	S5

* Corresponding author. Jian-Guo Zhang: zjgbit@bit.edu.cn
Junqing Yang: yjq881223@163.com

The mathematical forms for the parameters S_r , D , and t :

1. S_r index is defined as Eq(1):

$$S_r = \int S_r(r) dr \equiv \int \sqrt{\rho^{\text{hole}}(r)\rho^{\text{ele}}(r)} dr \quad (1)$$

Where the $\rho^{\text{hole}}(r)$ and $\rho^{\text{ele}}(r)$ denote the density distribution of hole and electron.

2. D index is defined as Eq(2):

$$D = |D| \equiv \sqrt{(X_{\text{ele}} - X_{\text{hole}})^2 + Y_{\text{ele}} - Y_{\text{hole}}^2 + Z_{\text{ele}} - Z_{\text{hole}}^2} \quad (2)$$

Taking X coordinate of centroid of electron (X_{ele}) as an example, X_{ele} is written as:

$$X_{\text{ele}} = \int x \rho^{\text{ele}}(r) dr$$

Where x is X component of position vector r .

3. t index is to measure separation of hole and electron in CT direction, which is defined as Eq(3):

$$t = D - H_{\text{CT}} \quad (3)$$

H_{CT} is written as:

$$H_{\text{CT}} = |H \cdot \mu_{\text{CT}}|$$

$$H = (|\sigma_{\text{ele}}| + |\sigma_{\text{hole}}|) / 2$$

Where μ_{CT} is unit vector in CT direction; $|\sigma_{\text{ele}}|$ and $|\sigma_{\text{hole}}|$ are refer to as σ_{hole} and σ_{ele} indices, they measure overall RMSD of hole and electron, respectively.

Table S1. Excitation descriptors (Sr , D , Sr/D , and t) and the statistical charge transfer data.

Complexes	Sr	D (Å)	Sr/D	t	M→L	L→M	L→L	MC	LC
1A	0.28	2.80	0.10	1.77	0.003	0.070	0.617		0.310
2A	0.49	2.53	0.19	1.17	0.049	0.405	0.334	0.039	0.172
3A	0.28	2.75	0.10	1.79		0.001	0.665		0.333
4A	0.30	3.67	0.08	2.65	0.002	0.023	0.079		0.947
5A	0.43	2.23	0.19	0.05	0.012	0.014	0.650		0.324
6A	0.26	3.70	0.07	2.60		0.008	0.010		0.982
1B	0.29	2.91	0.10	1.87	0.003	0.066	0.615		0.314
2B	0.36	3.60	0.10	2.06	0.013	0.210	0.152	0.004	0.618
3B	0.30	2.86	0.10	1.88		0.002	0.655		0.343
4B	0.31	3.64	0.08	2.60	0.001	0.025	0.029		0.944
5B	0.29	3.18	0.09	1.55		0.012	0.671		0.316
6B	0.31	3.59	0.09	2.50	0.001	0.018	0.059		0.922
7B	0.34	0.05	6.80	-3.28	0.013	0.004	0.861		0.119
8B	0.30	3.14	0.10	1.82	0.022	0.001	0.073		0.898
9B	0.55	1.90	0.29	0.42	0.550	0.026	0.233	0.039	0.152
10B	0.52	0.70	0.74	-1.24	0.294	0.038	0.325	0.017	0.326

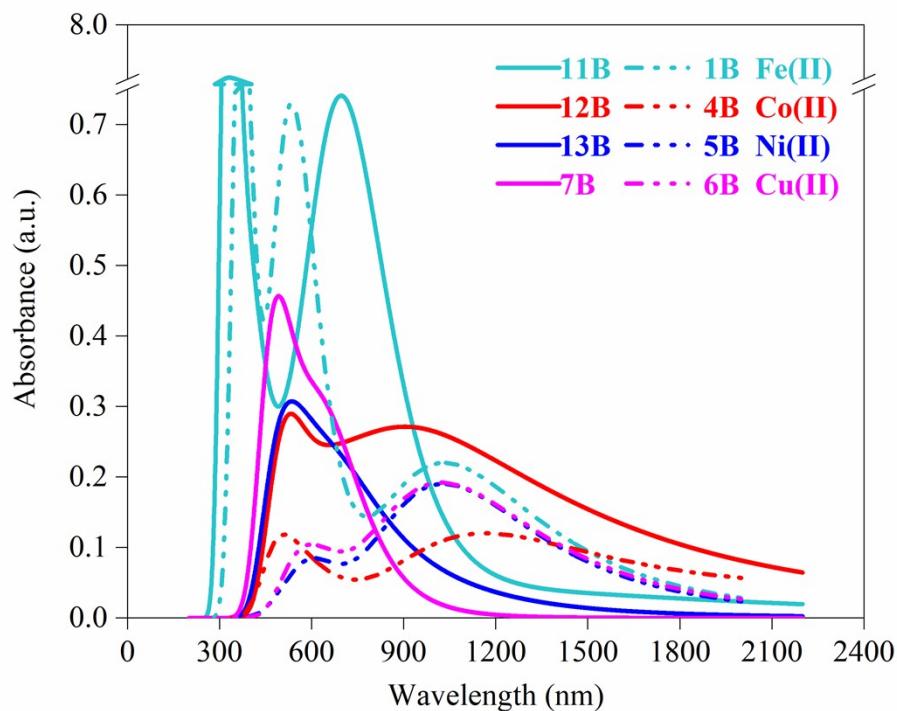


Figure S1. UV-vis spectra of NO_3^- (solid line) and non- NO_3^- (dotted line) bounded complexes.

Figure S1 shows the UV-vis absorption spectra of NO_3^- bounded complexes (**11B**, **12B**, **13B**, **7B**) with solid lines. For comparison, their non- NO_3^- bounded analogues (**1B**, **4B**, **5B**, **6B**) are also presented with dotted lines. There are several spectral differences between these two series. In the NO_3^- bounded complexes, the peak location of the low-energy CT band varies between 696 nm in **11B**, 904 nm in **12B**, 535 nm in **13B**, and 493 nm in **7B**. In the non- NO_3^- bounded complexes, it varies between 1031 nm in **1B**, 1166 nm in **4B**, 1029 nm in **5B** and 1021 nm in **6B**. Obviously, the CT band is blue-shifted in the NO_3^- bounded complexes relative to that of the non- NO_3^- analogues, while the absorption magnitude of the low energy CT band peaks is found to be larger in the former, which can be likely attributed to the effect of the NO_3^- on the electronegativity and electronic structure. Besides, in non- NO_3^- bounded analogues, Fe(II) complex (**1B**) possesses the strongest absorption intensity at 1064nm. However, in NO_3^- bounded complexes, Co(II) complex (**12B**) possesses the strongest absorption intensity at 1064nm. The anomalous behavior of **12B** may be attributed to the distributions of NO_3^- groups: in the same side for **12B**, while in the opposite sides for **7B**, **11B**, and **13B**.

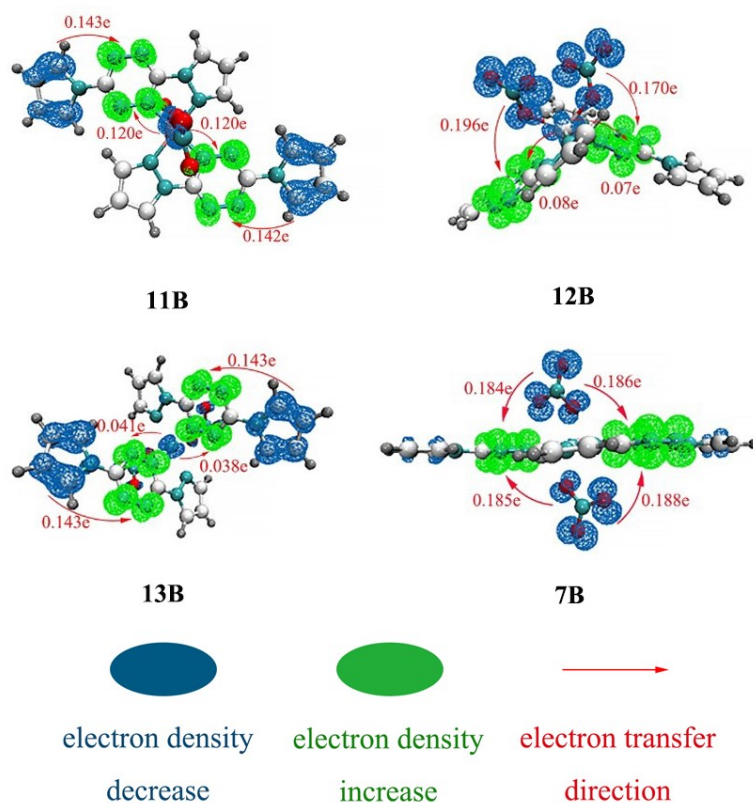


Figure S2. Charge density difference (CDD) plots of complexes **11B-13B** and **7B**.

Figure S2 shows the CDD plots of complexes **7B** and **11B-13B**. In comparison with the non- NO_3^- bounded divalent metal complexes, all the NO_3^- bounded complexes have relative obvious MLCT character, as TMD plots presented in the main manuscript. The electron transfers from metal to ligand are 0.013e (**7B**), 0.248e (**11B**), 0.158e (**12B**), and 0.081e (**13B**), respectively. The specific charge transfers in all transition modes of **7B** and **11B-13B** are in follows:

7B: MLCT 0.013, LMCT 0.004, LLCT 0.861, LC 0.119

11B: MLCT 0.248, LMCT 0.003, LLCT 0.409, MC 0.001, LC 0.332

12B: MLCT 0.158, LMCT 0.040, LLCT 0.760, MC 0.008, LC 0.034

13B: MLCT 0.081, LMCT 0.028, LLCT 0.506, MC 0.002, LC 0.379